**Journal of Mines, Metals and Fuels,** 71(1): 57-65; 2023. DOI: 10.18311/jmmf/2023/33357

Print ISSN : 0022-2755

Journal of Mines, Metals and Fuels

Contents available at: www.informaticsjournals.com/index.php/jmmf

# Effect of ECAP on Microstructure and Wear Resistance of AZ91 Magnesium Alloy

**Rajesh Yandigeri[1], Paresh S V[1], C Siddaraju[1] and Niranjan C A[2]**

*[1]Department of Mechanical Engineering, Ramaiah Institute of Technology, Bengaluru 560054, Karnataka.*
*E-mail: siddaraju80@gmail.com*
*[2]Department of Industrial Engineering and Management, Ramaiah Institute of Technology, Bengaluru 560054, Karnataka.*

## Abstract

*The present study aims to enhance the hardness and wear resistance of AZ91 Magnesium (Mg) alloy using Equal Channel Angular Pressing [ECAP]. Specimens were initially prepared using the die casting technique and were homogenized at 420°C for 24 hours. Both homogenized and non-homogenized specimens were subjected to an ECAP single pass under different temperatures. A Scanning Electron Microscope was used to study the influence of die heating temperature on the microstructure of AZ91 Mg alloy. A reciprocating wear test was carried out using the weight loss method to analyse the importance of ECAP on wear resistance. Results revealed that the microhardness and wear resistance of AZ91 were found to have increased after ECAP. Homogenization of specimens showed improved properties compared to non-homogenized specimens. Grain refinement was observed in both homogenized and non-homogenized samples. Cracks were observed on the ECAPed specimen when the ECAP temperature was maintained at 435°C–455°C. Overall, ECAP caused grain refinement, increased hardness and wear resistance in the AZ91 Mg alloy.*

***Keywords:*** *Microstructure, Wear Resistance, Machinability, Microhardness, Homogenized, ECAP.*

## 1.0 Introduction

The ever-increasing demand to decrease the weight of parts in the aerospace and automobile sectors has increased the interest in magnesium alloys as lightweight materials. Magnesium is lighter than aluminium and is used in various applications because of its low density, high specific strength, stiffness, superior damping capability, and machinability[1]. The AZ91 variant of Mg alloy is well known and is widely used in structural applications as it exhibits excellent corrosion resistance, casting characteristics and mechanical properties along with abundant availability in the commercial sector[2]. The ductility and formability of AZ91 alloy are poor because of its crystal structure being hexagonal close packed and the presence of secondary phases, which limit its use in the industrial applications[3]. Owing to their favourable engineering properties and most importantly because of their density, which is comparable to that of the human bone. Currently, magnesium alloys are used as biomaterials for the production of bio-absorbable implants and medical devices because of their harmless nature towards the human body as compared to several other structural materials[4]. The major disadvantage of magnesium is its low corrosion resistance. Low corrosion resistance results in the faster release of degradation products. A high rate of degradation can cause a reduction in the mechanical integrity of the implants before the bones are sufficiently healed[5,6]. Hence, there exists a need to improve the properties of magnesium alloys. Fine-grained AZ91 alloys can be obtained by severe plastic deformation (SPD). Among various SPD methods, Equal Channel Angular Pressing is the most widely used technique.

## 2.0 Methodology

AZ91 Mg alloy was produced using a die casting method, then the alloy was subjected to a machining process to

*Author for correspondence

obtain circular billets of a height of 45 mm and a diameter of 9 mm using wire EDM where the dielectric chosen was a combination of JR3A gel and demi water to ensure low conductivity and hence fine surface finish[7]. For homogenization, specimens were treated thermally in an electric heat furnace at a temperature of 420°C for 24 hours[8]. Thermally treated specimens are referred to as homogenized specimens, while thermally untreated specimens are referred to as non-homogenized specimens. To determine the effect of homogenization, the results were compared. Then, all the specimens were subjected to the ECAP secondary process using a die having a die insertion angle of 135° to ensure equivalent strain distribution[9] when pressed under a load of 15kN in UTM at a plunger velocity of 2mm/min. Different trials were conducted at different DIE temperatures. Fig.1 shows the 3D model of die used in present study which was designed using solidworks.

Figure 1: Die

# 3.0 Results and Discussion

## 3.1 Equal Channel Angular Pressing

In order to perceive the optimum temperature of processing the non-homogenized and homogenized AZ91 Mg alloy, trials at various die temperatures were conducted and the surface observations were recorded as shown in the tables below. Table 1 and Table 2 show the results obtained after passing non-homogenized and homogenized AZ91 Mg alloy through the ECAP die at different temperatures, respectively.

Observations from the tables show that the optimum temperatures for drawing processing the non-homogenized and homogenized AZ91 Mg alloy through equal channel angular pressing die with an insertion angle of 135° was found out to be 420°C and 425°C respectively.

**Table 1: Non-homogenized specimens after processing at different temperatures**

| Trial Number | Process Temperature | Condition of the specimen |
|---|---|---|
| 1 | Room Temperature | Fracture |
| 2 | 415°C | Small cracks |
| 3 | 420°C | No cracks |
| 4 | 425°C | Small cracks |
| 5 | 435°C | Moderate cracks |
| 6 | 445°C | Moderate cracks |
| 7 | 455°C | Moderate cracks |

**Table 2: Homogenized specimens after processing at different temperatures**

| Trial Number | Process Temperature | Condition of the specimen |
|---|---|---|
| 1 | Room Temperature | Fracture |
| 2 | 415°C | Small cracks |
| 3 | 425°C | No cracks |
| 4 | 435°C | Small cracks |

Figure 2: Non-homogenized AZ91 Mg alloy processed at 420°C

Figure 3: Homogenized AZ91 Mg alloy processed at 425°C

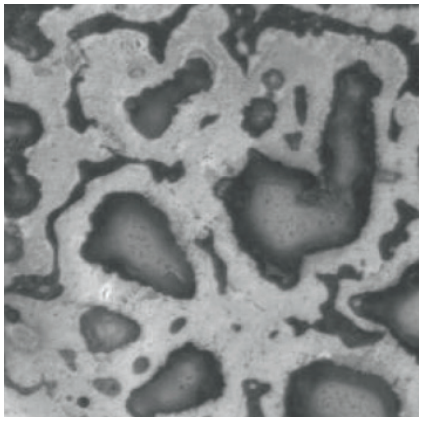

Figure 4: Microstructure of non-homogenized AZ91 Mg alloy after etching with the glycol

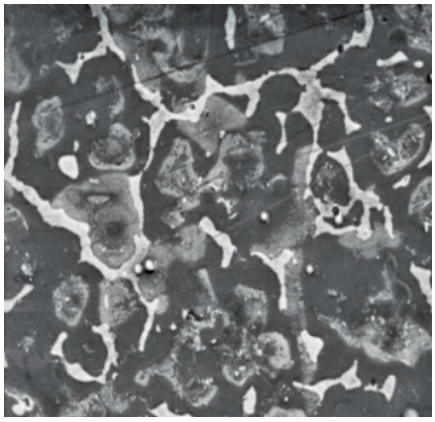

Figure 5: Microstructure of non-homogenized AZ91 Mg alloy after etching with the phospho-picral

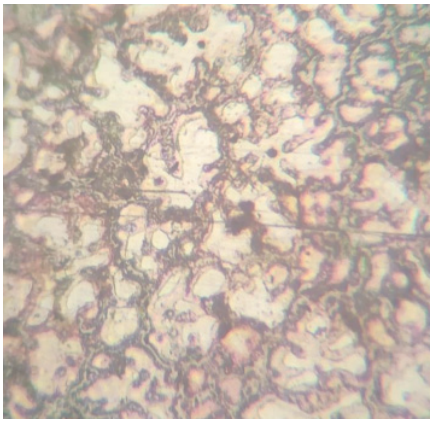

Figure 6: Microstructure of non-homogenized AZ91 Mg alloy after etching with the acetic-picral

## 3.2 Microstructure Characterization

Figures 4, 5, and 6 show the microstructure of non-homogenized AZ91 Mg alloy etched with different etchants. Fig.4 shows the microstructure of a non-homogenized AZ91 Mg alloy etched with glycol reagent[10]. It was observed that glycol etchant washes out grain boundaries, making it extremely difficult to distinguish between primary $\alpha$-Mg matrix, precipitate $\beta$-$Mg_{17}Al_{12}$ phase and divorced eutectic of $\alpha$+$\beta$. Fig. 5 shows the microstructure of the non-homogenized AZ91 Mg alloy etched with phospo-picral etch[11]. It is observed that phospo-picral darkens the massive $\alpha$-Mg matrix preferentially. It also brightens the $\beta$-$Mg_{17}Al_{12}$ phase, which slightly hinders the visibility of the $\alpha$+$\beta$ phase. Fig. 6 shows the microstructure of a non-homogenized AZ91 Mg alloy etched with acetic-picral etch[12]. It is observed that acetic-picral denaturates the $\beta$-$Mg_{17}Al_{12}$ phase, making the $\alpha$-Mg matrix appear lighter in comparison. It also reveals the grain boundaries better than the other two etchants.

Based on the results drawn from the comparison made using different etchants as discussed above, acetic-picral was chosen as a standard etchant for further studies. The following figures show the microstructure of non-homogenized and homogenized AZ91 Mg alloy etched with acetic-picral etchant, prior to the ECAP process. Fig.7 shows the microstructure of non-homogenized AZ91 Mg alloy etched with acetic-picral etchant. From the figure typical dendritic segregation in the microstructure of AZ91 Mg alloy can be observed, the coarse and reticular $\beta$-$Mg_{17}Al_{12}$ phases are distributed along with the original grain boundaries besides $\alpha$-Mg matrix to a large extent. The lighter coloured materials surrounds the dark $\beta$-$Mg_{17}Al_{12}$ phase, which is known as the divorced eutectic of $\beta$-$Mg_{17}Al_{12}$ phase while the $\alpha$-Mg, precipitate $\beta$-$Mg_{17}Al_{12}$ and divorced eutectic of $\alpha$+$\beta$ constitute the main phase of the microstructure. Fig.8 shows the microstructure of homogenized AZ91 Mg alloy etched with acetic-picral etchant. A large amount of variation in the amount and form of second phase along with, the decrease in the amount of $\beta$-$Mg_{17}Al_{12}$ phase near to grain boundaries and inside $\alpha$-Mg matrix can be observed.

Fig.9 shows the microstructure of non-homogenized AZ91 Mg alloy etched with acetic-picral after ECAP processing at 420ºC. It was observed that the amount of $\beta$-$Mg_{17}Al_{12}$ is similar to the specimen prior to the ECAP, with a great reduction in the $\alpha$+$\beta$ eutectic phase. The average grain size is reduced considerably in comparison with the microstructure prior to ECAP. While, Fig.10 shows the microstructure of homogenized AZ91 magnesium alloy etched with acetic-picral, after ECAP processing 425ºC. It was observed that the microstructures of specimens processed at 415ºC and 425ºC (No figures in the paper) had more amount of $\beta$-$Mg_{17}Al_{12}$ phase when compared to the microstructure of the specimen processed at 420ºC. All the specimens had very negligible amount of $\alpha$+$\beta$ eutectic phase. The average grain size was reduced considerably when compared to the specimen prior to ECAP process.

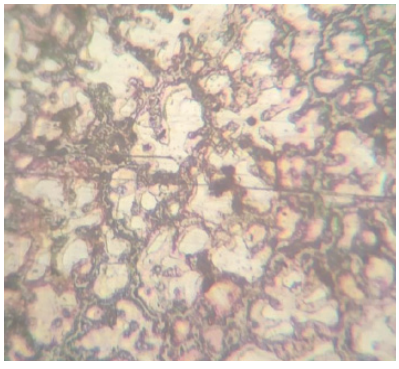

Figure 7: Microstructure of non-homogenized AZ91 Mg alloy etched with acetic-picral prior to ECAP process

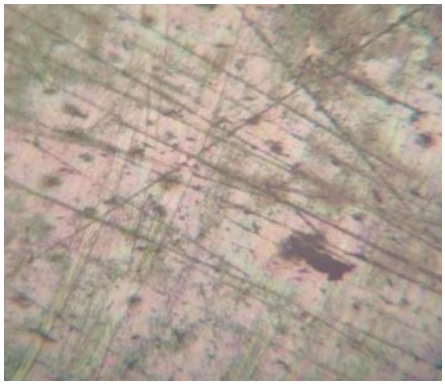

Figure 8: Microstructure homogenized AZ91 Mg alloy etched with acetic-picral prior to ECAP process

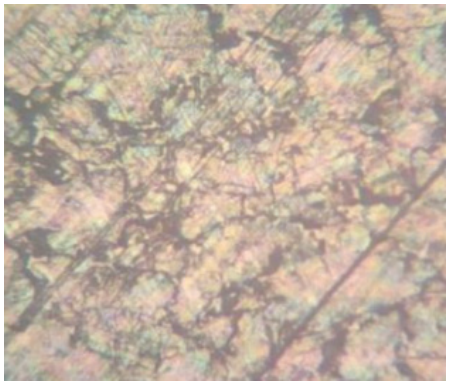

Figure 9: Microstructure of non-homogenized AZ91 Mg alloy etched with acetic-picral after ECAP processing 420ºC

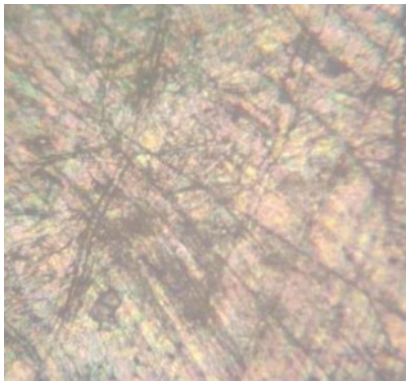

Figure 10: Microstructure of homogenized AZ91 Mg alloy etched with acetic-picral after ECAP processing at 425ºC

## 3.3 Microhardness

The following results have been obtained for homogenized and non-homogenized AZ91 magnesium alloy specimens prior to ECAP.

It is observed that, for the as-cast AZ91 Mg alloy specimen, the microhardness is 47.9±5.3 Hv. Microhardness increased to 77.3±11.2 Hv for the homogenized specimen. There is an increase of about 61.37% in the microhardness value of homogenized specimens when compared to non-homogenized specimens.

The following results have been obtained for non-homogenized AZ91 Mg alloy specimens after ECAP processing at different temperatures.

It is observed that, after ECAP processing at 415ºC, microhardness of the alloy increased to 107±8 Hv i.e. an increase of about 123.38% when compared to the specimen prior to ECAP. The microhardness of the specimens after ECAP processing at 420ºC and 425ºC is observed to be 108±5 Hv and 106±7 Hv, respectively. It is to be noted that, there is a marginal variation in the microhardness values for the specimens ECAP processed at 415ºC, 425ºC and 435ºC. The microhardness of the specimen after ECAP processing at 435ºC is observed to be 118±17 Hv, which is an increase of about 146.34% when compared to the specimen prior to ECAP, and an increase of about 9.26% when compared to the specimen ECAP processed at 415ºC.

The following results have been obtained for homogenized AZ91 Mg alloy specimens after ECAP processing at different temperatures.

**Table 3: Microhardness number of homogenized and non-homogenized AZ91 Mg alloy specimens prior to ECAP**

| Specimen | Microhardness Number (Hv) |
|---|---|
| Non-Homogenized | 47.9±5.3 |
| Homogenized | 77.3±11.2 |

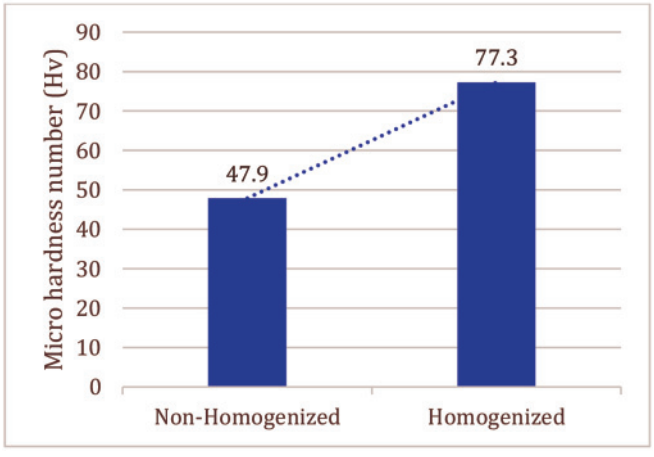


Figure 11: Graph showing microhardness number of homogenized and non-homogenized AZ91 Mg alloy specimens prior to ECAP process

**Table 4: Microhardness number of non-homogenized AZ91Mg alloy specimens after ECAP processing at different temperatures**

| Process Temperature | Microhardness Number(Hv) |
|---|---|
| 415ºC | 107±8 |
| 420ºC | 108±5 |
| 425ºC | 106±7 |
| 435ºC | 118±17 |
| 445ºC | 119±9 |
| 455ºC | 120±17 |

It is observed that, after ECAP processing at 415ºC, microhardness of the alloy increased to 111±5 Hv i.e. an increase of about 43.6% when compared to the specimen prior to ECAP, and an increase of about 3.74% when compared to the non-homogenized specimen processed at the same temperature. The microhardness of the specimens after ECAP processing at 425ºC and 435ºC is observed to be 113±6 Hv and 113±8 Hv, respectively. For both the specimens, there is an increase of about 1.8% in microhardness values when compared to the specimen processed at 415ºC. It is to be noted that there is a negligible change in microhardness values for the specimens ECAP processed at 425ºC and 435ºC.

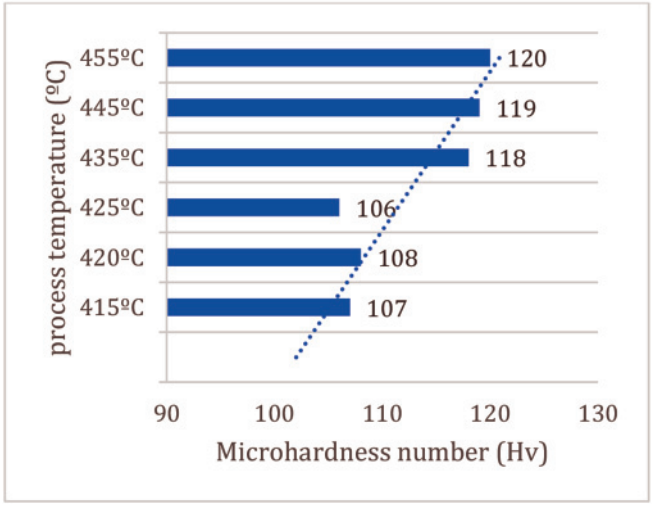


Figure 12: Graph showing microhardness number of non-homogenized AZ91 Mg alloy specimens after ECAP processing at different temperatures

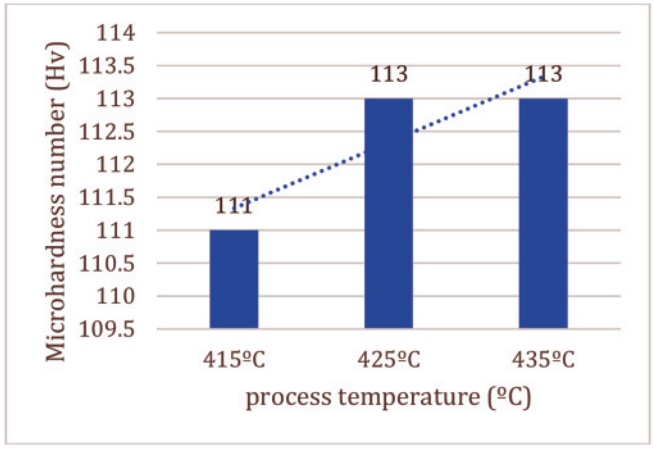


Figure 13: Graph showing microhardness number of homogenized AZ91 Mg alloy specimens after ECAP processing at different temperatures

**Table 5: Microhardness Number of homogenized AZ91 Mg alloy specimens after ECAP processing at different temperatures**

| Process temperature | Microhardness number (Hv) |
|---|---|
| 415ºC | 111±5 |
| 425ºC | 113±6 |
| 435ºC | 113±8 |

## 3.4 Wear Rate

The following results have been obtained for different specimens tested through the Linear Reciprocating Wear Tester for load 15 N, stroke 10 mm, time 45 min.

Table 6 shows wear conditions defined for specimens. In which load and stroke length were maintained constant and velocity and time were varied at 2 levels. From the previous studies it is indicated that velocity and time has significant influence on wear rate. Hence in the present study only velocity and time parameters are varied and load and stroke

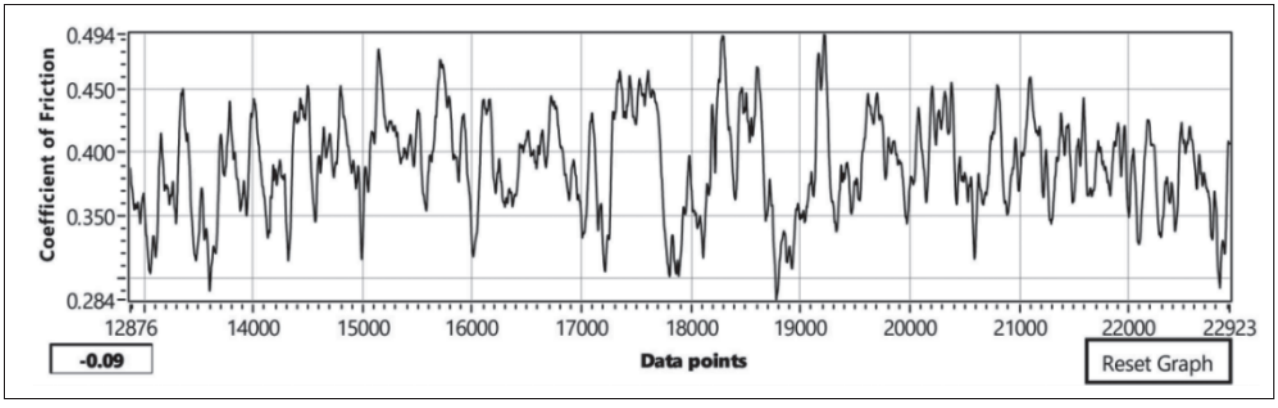


Figure 14: Graph for frequency of 4 Hz for non homogenized specimens prior to ECAP process

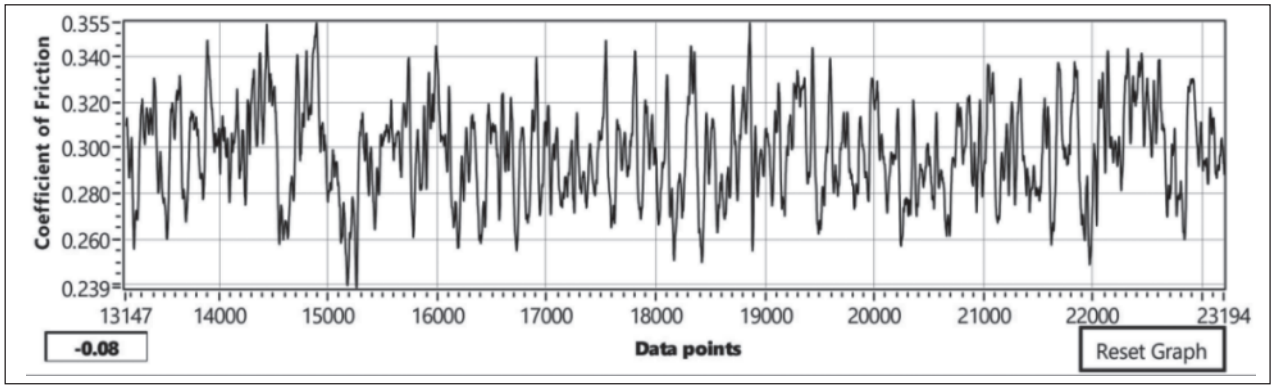


Figure 15: Graph for frequency of 6 Hz for non-homogenized specimens prior to ECAP process

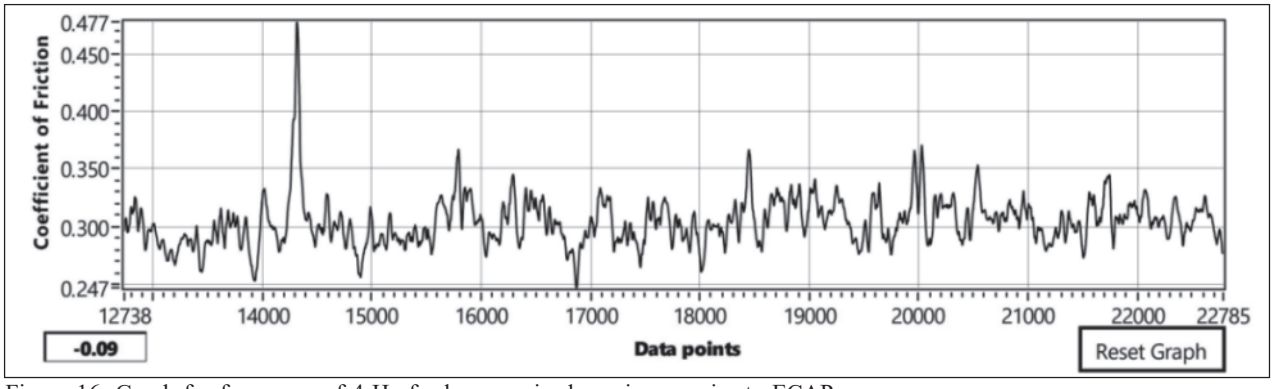


Figure 16: Graph for frequency of 4 Hz for homogenized specimens prior to ECAP process

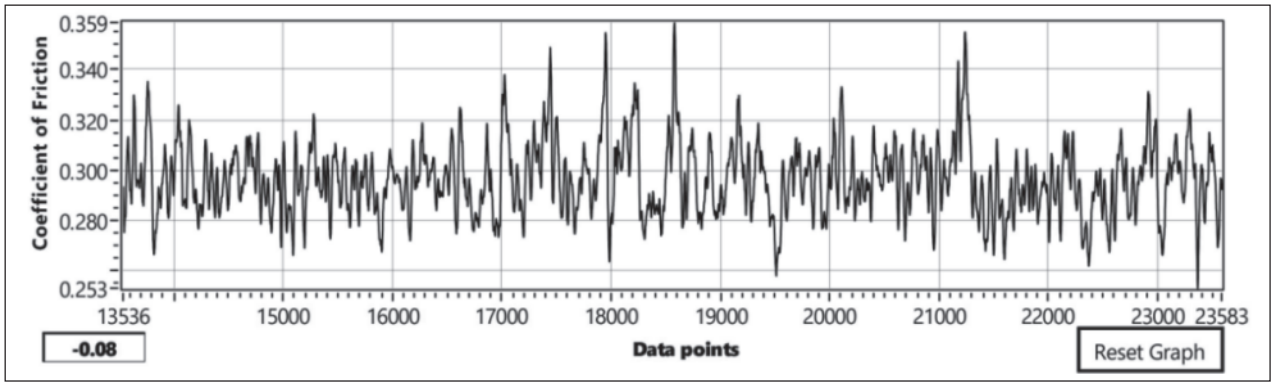


Figure 17: Graph for frequency of 6 Hz for homogenized specimens prior to ECAP process

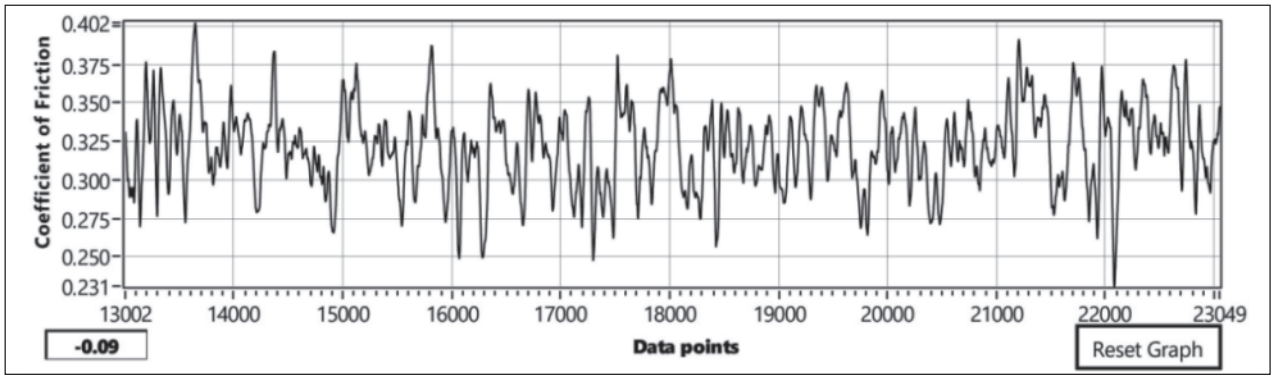


Figure 18: Graph for frequency of 4 Hz for non-homogenized specimens after ECAP processing at 420ºC

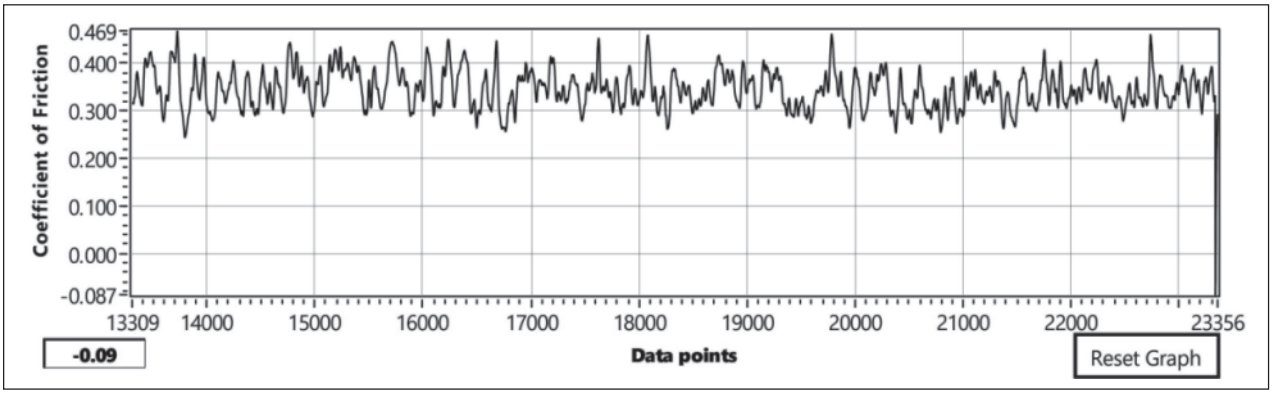


Figure 19: Graph for frequency of 6 Hz for non-homogenized specimens after ECAP processing at 420ºC

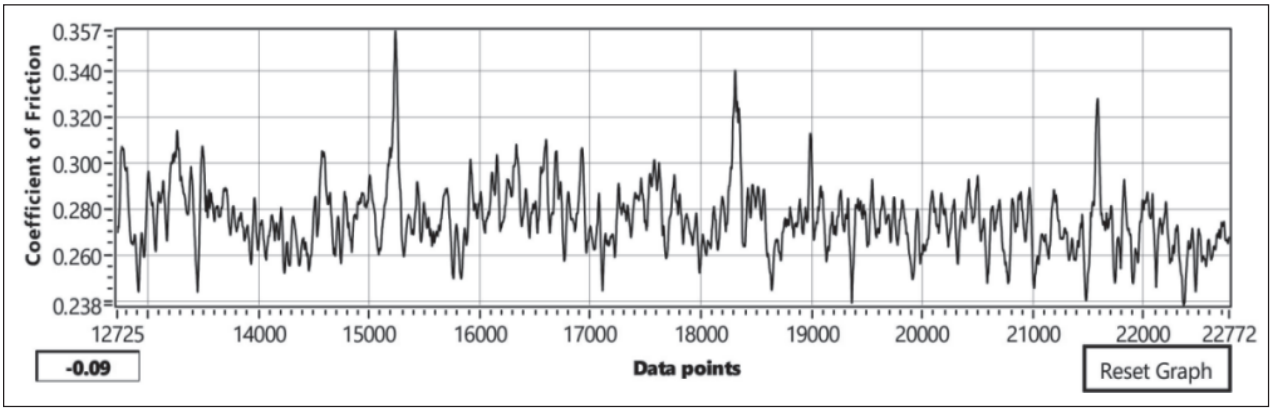


Figure 20: Graph for frequency of 4 Hz for homogenized specimens after ECAP processing at 425ºC

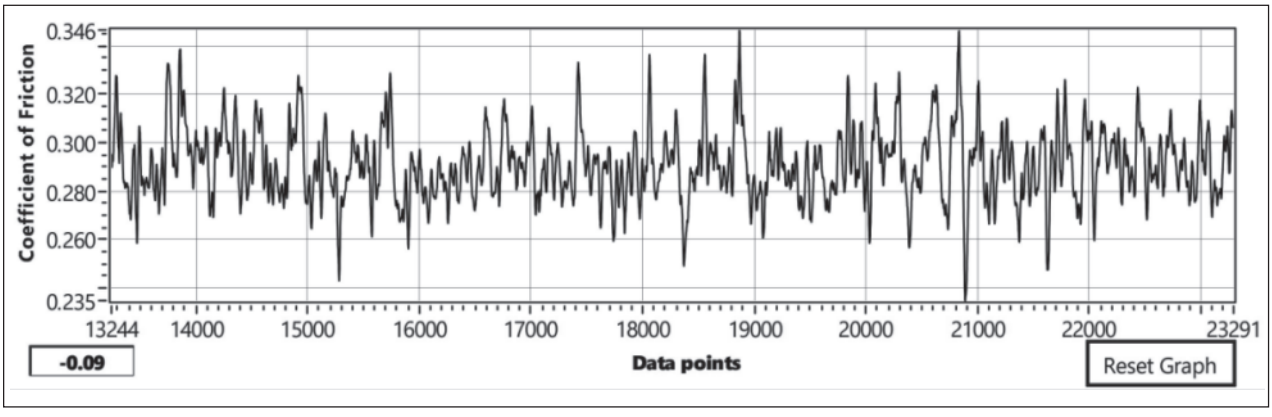


Figure 21: Graph for frequency of 6 Hz for homogenized specimens after ECAP processing at 425ºC

were kept constant. From the results it can be observed that homogenized specimens have better wear resistance compared to non-homogenized specimens before ECAP. This may be attributed because homogenized samples reported with increased hardness. Therefore homogenized samples have developed resistance to wear.

Contrary to these results after ECAP homogenized specimens were resulted in increase in wear rate compared to non-homogenized specimens. That is wear rate of specimens after ECAP was increased from 0.46 to 0.47 and 0.60 to 0.70. This can be attributed due to increase in ductility of the specimens after ECAP. Reduction in hardness values after homogenization and ECAP thus affected wear rate. i.e increase in wear rate. It can be concluded that ECAP after homogenization induces grain refinement and increases the ductility.

**Table 6: wear rate of specimens under different conditions**

| Wear rate of non-homogenized specimens prior to ECAP process | | | | | | | | | |
|---|---|---|---|---|---|---|---|---|---|
| Load (N) | Stroke (mm) | Frequency (Hz) | Velocity (mm/sec) | Time (min) | Weight at start (gm) | Weightat end (gm) | Loss of Weight (gm) | % wt. loss | Wear rate ($mm^2/N$) |
| 15 | 10 | 4 | 80 | 45 | 1.2505 | 1.2444 | 0.0061 | 0.48 | $10.135 \times 10^{-7}$ |
| 15 | 10 | 6 | 120 | 45 | 1.2375 | 1.2293 | 0.0082 | 0.66 | $9.320 \times 10^{-7}$ |
| Wear rate of homogenized specimens prior to ECAP process | | | | | | | | | |
| Load (N) | Stroke (mm) | Frequency (Hz) | Velocity (mm/sec) | Time (min) | Weight at start (gm) | Weightat end (gm) | Loss of Weight (gm) | % wt. loss | Wear rate ($mm^2/N$) |
| 15 | 10 | 4 | 80 | 45 | 1.3447 | 1.3394 | 0.0053 | 0.39 | |
| 15 | 10 | 6 | 120 | 45 | 1.3394 | 1.3310 | 0.0084 | 0.62 | |
| Wear rate of non-homogenized specimens after ECAP processing at 420ºC | | | | | | | | | |
| Load (N) | Stroke (mm) | Frequency (Hz) | Velocity (mm/sec) | Time (min) | Weight at start (gm) | Weightat end (gm) | Loss of Weight (gm) | % wt. loss | Wear rate ($mm^2/N$) |
| 15 | 10 | 4 | 80 | 45 | 1.1898 | 1.1843 | 0.0055 | 0.46 | |
| 15 | 10 | 6 | 120 | 45 | 1.1843 | 1.1771 | 0.0072 | 0.60 | |
| Wear rate of homogenized specimens after ECAP processing at 425ºC | | | | | | | | | |
| Load (N) | Stroke (mm) | Frequency (Hz) | Velocity (mm/sec) | Time (min) | Weight at start (gm) | Weightat end (gm) | Loss of Weight (gm) | % wt. loss | Wear rate ($mm^2/N$) |
| 15 | 10 | 4 | 80 | 45 | 1.1712 | 1.1656 | 0.0056 | 0.47 | |
| 15 | 10 | 6 | 120 | 45 | 1.1656 | 1.1574 | 0.0082 | 0.70 | |

## 4.0 Conclusions

In the present work, homogenized and non-homogenized samples of AZ91 Mg alloy were processed by ECAP with a die having an insertion (internal) angle (Φ) of 135º between two channels. The process was carried out only by a single pass. All the samples were attempted to be processed at temperatures below the solidus temperature. Microstructural characterization was carried out at each stage of processing. Mechanical properties were assessed before and after ECAP processing. Wear properties were evaluated before and after ECAP processing. The exposure obtained when picric acid was used as an etchant gave better results compared to that of glycol and phospho-picral acid, as the picric acid did not react with the alloying elements of AZ91 Magnesium alloy. Based on the experimental results obtained and the discussion presented, the following conclusions are drawn.

- The samples of AZ91 magnesium alloy processed by ECAP at room temperature were fractured, while the samples processed by ECAP after supplying constant heat to the die were not.
- The samples processed by ECAP at a lower temperature range (415ºC-425ºC) had fewer cracks when compared to the samples processed at a higher temperature range (435ºC-455ºC).
- 420ºC was found to be the optimum ECAP processing temperature for non-homogenized AZ91 Magnesium alloy samples, whereas 425ºC was found to be the optimum ECAP processing temperature for homogenized AZ91 Magnesium alloy samples, as no cracks were observed after a single pass.
- The microhardness of non-homogenized AZ91 Magnesium alloy sample was increased by 61.37% after the homogenization process.
- The microhardness of non-homogenized AZ91 Magnesium alloy samples after ECAP processing was increased by up to 146.34% when compared to the non-homogenized sample prior to ECAP processing, while the microhardness of homogenized AZ91 Magnesium alloy samples after ECAP processing was increased by up to 46.18% when compared to the homogenized sample prior to ECAP processing.

- When compared to the non-homogenized sample prior to ECAP processing, the wear rate of non-homogenized AZ91 Mg alloy sample processed by ECAP at 420ºC was reduced by 12.38%, while the wear rate of homogenized AZ91 Mg alloy sample processed by ECAP at 425ºC was reduced by 2.38%.

## 5.0 References


1. Kaveh Meshinchi Asl, (2011): School of Materials Science and Engineering, Clemson University, Clemson USA, Improving the Properties of Magnesium Alloys for High Temperature Applications, 6 June 2011.
2. Hemendra Patle, B Ratna Sunil and Ravikumar Dumpala, (2020): Sliding wear behaviour of AZ91/B4C surface composites produced by friction stir processing, 27 January 2020.
3. Zhenquan Yang 1, Aibin Ma 1, 2, Huan Liu 1, 3ORCID, Jiapeng Sun 1, ORCID, Dan Song 1, Ce Wang 1,Yuchun Yuan 1 and Jinghua Jiang 1, (2018): Multimodal Microstructure and Mechanical Properties of AZ91 Mg Alloy Prepared by Equal Channel Angular Pressing plus Aging, 26 September 2018.
4. Prof. Emanuela Cerri, Department of Industrial Engineering University of Parma, Italy. Prof. Nuno M. Neves, Department of Polymer Engineering, University of Minho, Portugal. Prof. Antonella Motta, Department of Industrial Engineering, University of Trento, Italy, Biodegradable stents made of pure Mg and AZ91 alloy through SPS sintering.
5. Long Liu, Fulai Yuan, Mingchun Zhao, Chengde Gao, Pei Feng, Youwen Yang, Sheng Yang and Cijun Shuai, (2017): Rare Earth Element Yttrium Modified Mg-Al-Zn Alloy, Microstructure, Degradation Properties and Hardness, 28 Apr 2017.
6. Fatemeh Zahra Akbarzadeh, Erfan Rezwani Ghomi, Seeram Ramakrishna, (2022): Improving the corrosion behaviour of magnesium alloys with a focus on AZ91 Mg alloy intended for biomedical application by microstructure modification and coating.
7. YS Liao, JT Huang, YH Chen, (2004): A study to achieve a fine surface finish in wire EDM.
8. Xingchuan Xia, Weimin Zhao, Xiangzheng Feng, Hui Feng, Xin Zhang, (2013): Effect of homogenizing heat treatment on the compressive properties of closed cell Mg alloy foams.
9. Atul Dayal, Ankit Sahai, K Hans Raj, Rahul Swarup Sharma, (2018): Comprehensive study of effect of processing parameters in ECAP, April 2018.
10. Z Trojanova, V Gartnerova, A Jager, A Namesny, M Chalupova, P Placek, P lukac, Mechanical and fracture properties of AZ91 Magnesium alloy reinforced by Si and SiC particles.
11. Tianping Zhu, Zhan W Chen, Wei Gao, Microstructure formation in partially melted zone during gas tungsten arc welding of AZ91 Mg cast alloy, 2008.
12. Yutaka S Sato, A Sasaki, A Sugimoto, Honda, Hiroyuki Kokawa, Enhancement of formability in magnesium alloy AZ31B via friction stir casting processing.